J Neurooncol (2016) 128:47–56
DOI 10.1007/s11060-016-2098-9

LABORATORY INVESTIGATION

Preservation of *KIT* genotype in a novel pair of patient-derived orthotopic xenograft mouse models of metastatic pediatric CNS germinoma

Holly Lindsay[1] · Yulun Huang[2] · Yuchen Du[1] · Frank K. Braun[1] · Wan Yee Teo[3] · Mari Kogiso[1] · Lin Qi[1] · Huiyuan Zhang[1] · Sibo Zhao[1] · Hua Mao[1] · Frank Lin[1] · Patricia Baxter[1] · Jack M. Su[1] · Keita Terashima[4] · Laszlo Perlaky[1] · Murali Chintagumpala[1] · Adekunle Adesina[5] · Ching C. Lau[1] · D. Williams Parsons[1] · Xiao-Nan Li[1]

Received: 4 December 2015 / Accepted: 15 February 2016 / Published online: 8 March 2016

Abstract Metastatic intracranial germinoma is difficult to treat. Although the proto-oncogene *KIT* is recognized as one of the most frequent genetic abnormalities in CNS germinoma, the development of new target therapeutic agents for CNS germinoma is hampered by the lack of clinically-relevant animal models that replicate the mutated or over-expressed KIT. CNS germinoma tumor cells from five pediatric patients were directly implanted into the brains of Rag2/severe combined immune deficiency mice. Once established, the xenograft tumors were sub-transplanted in vivo in mouse brains. Characterization of xenograft tumors were performed through histologic and immunohistochemical staining, and KIT mutation analysed with quantitative pyro-sequencing. Expression of putative cancer stem cell markers (CD133, CD15, CD24, CD44, CD49f) was analyzed through flow cytometry. Two patient-derived orthotopic xenograft (PDOX) models (IC-6999GCT and IC-9302GCT) were established from metastatic germinoma and serially sub-transplanted five times in mouse brains. Similar to the original patient tumors, they both exhibited faint expression (+) of PLAP, no expression (−) of β-HCG and strong (+++) expression of KIT. *KIT* mutation (D816H), however, was only found in IC-9320GCT. This mutation was maintained during the five in vivo tumor passages with an increased mutant allele frequency compared to the patient tumor. Expression of putative cancer stem cell markers CD49f and CD15 was also detected in a small population of tumor cells in both models. This new pair of PDOX models replicated the key biological features of pediatric intracranial germinoma and should facilitate the biological and pre-clinical studies for metastatic intracranial germinomas.

Keywords Mouse models · Germinoma · Pediatric · KIT · Xenograft

✉ Xiao-Nan Li
xxli@txch.org

[1] Department of Pediatrics, Baylor College of Medicine/Texas Children's Cancer Center, 1102 Bates, Suite 1030.07, Houston, TX 77030, USA

[2] Department of Neurosurgery, The 1st Affiliated Hospital, Soochow University, Suzhou, Jiangsu 215007, People's Republic of China

[3] Humphrey Oei Institute of Cancer Research, National Cancer Center Singapore, 11 Hospital Drive, Singapore 169610, Singapore

[4] Children's Cancer Center, National Center for Child Health and Development, 2-10-1 Okura Setagaya-ku, Tokyo 157-8535, Japan

[5] Department of Pathology, Baylor College of Medicine/Texas Children's Hospital, 6621 Fannin Street, Houston, TX 77030, USA

Introduction

Intracranial germ cell tumors (GCTs) comprise 3–15 % of pediatric brain tumors and can be sub-classified into pure germinomas (2/3 of cases) and non-germinomatous germ cell tumors based on histopathology and serum and cerebral spinal fluid (CSF) biomarkers [1–5]. Although survival rates for exceed 75 %, curative therapies come with significant morbidities, and salvage rates after relapse are as low as 50 % [1, 2].

Recent studies have identified the proto-oncogene *KIT* as one of the most frequent genetic abnormalities in CNS germinoma [3, 6–8]. When constitutively activated by mutations or amplification, *KIT* induces uncontrolled ligand-independent cellular proliferation and resistance to

apoptosis [9, 10]. *KIT* mutation has been reported in up to 55 % of CNS germinomas, with the majority occurring in chromosome 4 codon 816. In addition to mutation, KIT over-expression is a pathologic characteristic of CNS germinoma [3, 6–8].

For CNS germinoma, there are neither cell lines nor animal models that replicate the mutated *KIT* and/or over-expressed KIT seen in patient tumors. To meet the critical need for in vivo model systems in pediatric neuro-oncology, our laboratory has successfully developed over 70 orthotopic xenograft models of seven tumor pathologies from patient surgical specimens. Many of these patient-derived orthotopic xenograft (PDOX) models have been extensively characterized and maintain molecular and genetic fidelity with the model-initiating human tumors [11, 12].

We consequently set out to explore whether clinically-relevant PDOX models could be developed from fresh surgical specimens of pediatric germ cell tumors. In this report, we describe the establishment and characterization of two PDOX models of metastatic pediatric CNS germinoma. We hypothesized that these models would replicate the original human tumors' pathologic and immunohistochemical signatures and serve as biologically-accurate models for future pre-clinical investigations.

Materials and methods

Tumor specimens

Tumor specimens were obtained from five patients with intracranial germ cell tumors treated at Texas Children's Hospital. Signed informed consent was obtained from each legal guardian prior to sample acquisition in accordance with local Institutional Review Board policy. The patients' clinical characteristics and outcomes are described in Table 1.

Freshly resected metastatic pure germinoma from C6 spinal cord was obtained from the first patient at the time of tumor recurrence and labelled 6999GCT [3]. This metastatic tumor sample utilized for model establishment was obtained 9 months after initial biopsy of the primary tumor and following treatment with chemotherapy and radiation. Tumor tissue was washed and minced with fine scissors. Single tumor cells were collected with a 40 μm strainer and re-suspended in Dulbecco's modified Eagle's medium (DMEM) to achieve a concentration of 1×10^8 live cells/mL on trypan blue staining.

Metastatic CSF tumor cells were obtained from the second patient and labelled 9320GCT [3]. The diagnosis of pure germinoma was made from the resected primary supratentorial tumor mass; unfortunately, no primary site

Table 1 Clinical characteristics and outcomes of patients used to establish PDOX models

Tumor ID	Diagnosis	Age/sex	CSF markers AFP	CSF markers β-HCG	Source of cells for implantation	Treatment	Response/outcome
6999	Germinoma	16 years/M	<1	18	Metastasis (C6 spinal cord)	Surgical resection, XRT, chemo	Progression/Alive at 3 years
9320	Germinoma	1.5 years/F	<1	<1	Metastasis (CSF)	Surgical resection, chemo	Progression/died at 10 weeks
2597	Germinoma	8 years/F	<1	46	Primary site (pituitary)	Surgical resection, XRT, chemo	Complete response/alive at 2.5 year
2655	NGGCT	12 years/M	5	582	Primary site (pineal gland)	Chemo, XRT	Partial response/alive at 5 year
9806	Immature teratoma and yolk sac	12 years/M	<1	<1	Primary site (pineal gland)	Surgical resection, XRT, chemo	Progression/lost to follow-up after surgery

AFP α-fetoprotein (ng/mL), *β-HCG* β-human chorionic gonadotropin (IU/L), *chemo* chemotherapy, *CSF* cerebrospinal fluid, *NGGCT* non-germinomatous germ cell tumor, *XRT* radiation therapy

tissue was available for research. The patient had received no treatment prior to tissue acquisition.

Primary site tumor samples were obtained from the remaining three patients and processed as described above. All samples were subsequently transferred on ice to the animal facility for intracranial implantation.

Orthotopic transplantation of human tumor cells into mouse cerebra

Rag2/severe combined immune deficiency (SCID) mice were bred and housed in a pathogen-free animal facility. All animal experiments were conducted according to an Institutional Animal Care and Use Committee-approved protocol. Surgical transplantation of tumor cells into mouse cerebrum was completed via our previously described protocol [11, 12]. Briefly, mice aged 6–8 weeks were anesthetized with sodium pentobarbital (50 mg/kg, intraperitoneal). Tumor cells (1×10^5) suspended in 2 μL of culture medium were injected into the right cerebral hemisphere (1 mm to right of midline, 1.5 mm anterior to lambdoidal suture, 3 mm deep) via a 10 μL 26-gauge Gastight 1701 syringe needle (Hamilton Company).

Serial tumor sub-transplantation in vivo in mouse brains

Whole murine brains containing visible intra-cerebral (IC) tumors were aseptically removed and transferred to the tissue culture laboratory. Tumors were microscopically dissected from surrounding brain tissue, mechanically dissociated into cell suspensions, and filtered. Single tumor cells were subsequently injected into the brains of SCID mice as described above. For models IC-6999GCT and IC-9320GCT, the sub-transplantation process was repeated to complete a total of five tumor passages. In addition, injections of only 1×10^3 and 1×10^4 as well as the standard 1×10^5 tumor cells were performed for passage 5 of IC-9320GCT to determine the impact of implanted tumor cell number on xenograft survival.

Histologic and immunohistochemical characterization of xenograft tumors

After the development of neurologic deficits or once 12 months had passed following tumor implantation, mice were euthanized. Whole brains were aseptically removed and embedded in paraffin. Brains from models IC-6999GCT and IC-9320GCT at various passages were serially sectioned (5 mm thickness per slice) and stained with hematoxylin and eosin (H&E) following standard protocol.

Immunohistochemical (IHC) staining was performed using a Vectastain Elite kit (Vector Laboratories) [11, 12]. Primary antibodies included human-specific mitochondria (1:50) (Chemicon International), β-human chorionic gonadotropin (β-HCG) (Biomedia), placental alkaline phosphatase (PLAP) (Dako), and CD117 (KIT) (AB-1, Oncogen Science) [13]. After slides were incubated with primary antibodies for 90 min, the appropriate biotinylated secondary antibodies (1:200) were applied and incubated for 30 min. The final signal was developed using the 3,3′-diaminobenzidine substrate kit for peroxidase.

Pyrosequencing

Pyrosequencing was performed to detect *KIT* mutations using the following primers to amplifying a 134-bp genomic fragment spanning the codon 816 sequence of *KIT*: Forward 5′-TTGGCAGCCAGAAATATCCTCC-3′, reverse 5-Bio-CTGTCAAGCAGAGAATGGGT-3′. PCR was performed using AmpliTaq Gold (Roch) under standard conditions with 50 ng of DNA template in 50 μL. After the amplified PCR product was checked by gel electrophoresis, pyrosequencing was performed on a PSQ 96 (Qiagen). 40 μL of PCR product, 3 μL Streptavidin Sepharose High Performance beads, and 40 μL of binding buffer were well mixed in a 96 well plate. PCR products attached to the beads were washed and subsequently denatured in 0.2 Normal NaOH. Purified DNA samples were annealed to the sequencing primer (0.3 μM) and denatured for 5 min at 85 °C; samples were then processed in the PSQ 96 instrument. The sequence was analyzed using following dispensation order: GAGTAG**X**ACA. Incorporation of a non-wild type nucleotide at position 7 with allelic frequency >10 was considered positive for mutation.

Flow cytometry analysis of putative germinoma stem cell markers

Flow cytometry analysis using LSR II (BD Biosciences) was performed to quantify the presence of candidate stem cell surface markers in the PDOX models. Single cell suspensions were stained with propidium iodine to gate out dead cells and with a four antibody anti-mouse cocktail (CD90.1, CD133, CD140a, and CD24 conjugated to allophycocyanin (Biolegend)) to gate out murine cells. Staining was then done with CD133 and CD44 antibodies conjugated to phycoerythrin and CD15, CD24, and CD49f antibodies each conjugated to FITC (MACS Miltenyi Biotec). Cells and antibodies were incubated at 4 °C prior to re-suspension in a mixture of Dulbecco's Phosphate-Buffered Saline (Corning), bovine serum albumin (Sigma), and ethylenediaminetetraacetic acid (GIBCO-Invitrogen).

Analysis of flow data was performed using Kaluza Analysis Software (Beckman Coulter).

Statistical analysis

Animal survival times were evaluated by log-rank analysis followed by pairwise multiple comparison procedures using the Holm-Sidak method with SigmaPlot 13 (Systat Software).

Results

Two metastatic germinomas formed transplantable xenograft tumors in mouse brains

Implanted germinoma cells obtained from metastatic sites (patient tumors 6999GCT and 9320GCT) successfully formed intra-cerebral xenografts (designated IC-6999GCT and IC-9320GCT) to constitute tumor passage 1. At passage 1, xenograft tumors formed in 4 of 6 implanted mice for IC-6999GCT (67 % tumor take rate) and in all nine implanted mice for IC-9320GCT (100 %). Cells from both models maintained their in vivo tumorigenicity over four serial sub-transplantations to complete five total tumor passages as documented either by grossly visible tumors upon brain harvesting or on histopathologic analysis of paraffin-embedded, serially-sectioned brains. In both models, 100 % of implanted mice formed tumors in passages 3 and 5.

In contrast, however, no xenograft tumors formed from implanted patient tumors 2597GCT, 2655GCT, or 9806GCT. Although sample size is small, these data suggest that tumor cells obtained from metastatic sites are more biologically "aggressive" than those from the primary site and thus better able to form transplantable tumors.

For both PDOX models, animal survival times were monitored over all 5 tumor passages in mice implanted with identical numbers of tumor cells (1×10^5) to examine the reproducibility of tumor growth rates (Fig. 1). In IC-6999GCT, average xenograft survival decreased significantly from passage 1–2 ($p < 0.05$) but subsequently stabilized, with an average median survival in passage 1 of 263 days compared to 155 days in passages 2–5 (Fig. 1a). In IC-9320GCT, the overall animal survival times were similar, particularly in passages 2 through 5 ($p > 0.05$) (Fig. 1b). This stabilization in animal survival times in passages 2 through 5 is in agreement with what we have observed in our other established pediatric brain tumor PDOX models and suggests that tumor growth velocity is not significantly altered over serial tumor sub-transplantations beyond passage 1 [11, 12, 14].

Mice bearing IC-9320GCT xenografts had significantly shorter median survival (53 days) than those implanted with IC-6999GCT (263 days in passage 1 and 155 days from passage 2–5). One explanation is that model IC-9320GCT originated from relatively pure CSF metastatic tumor cells, while the C6 spinal cord solid tumor metastasis used for IC-6999GCT establishment likely contained not only germinoma cells but also normal human stromal cells that did not grow following implantation; consequently, the selective in vivo growth and subsequent enrichment of the germinoma tumor cell likely accounts for the decreased animal survival times in passages 2–5. Of note, the significantly shorter survival of IC-9320GCT xenografts compared to IC-6999GCT corresponds to the respective patients' outcomes, as patient 9320 died within 10 weeks of diagnosis and patient 6999 lived at least 3 years following initial therapeutic intervention.

In passages 2–5, IC-6999GCT xenograft tumors yielded an average of 1.02×10^7 live cells per tumor while

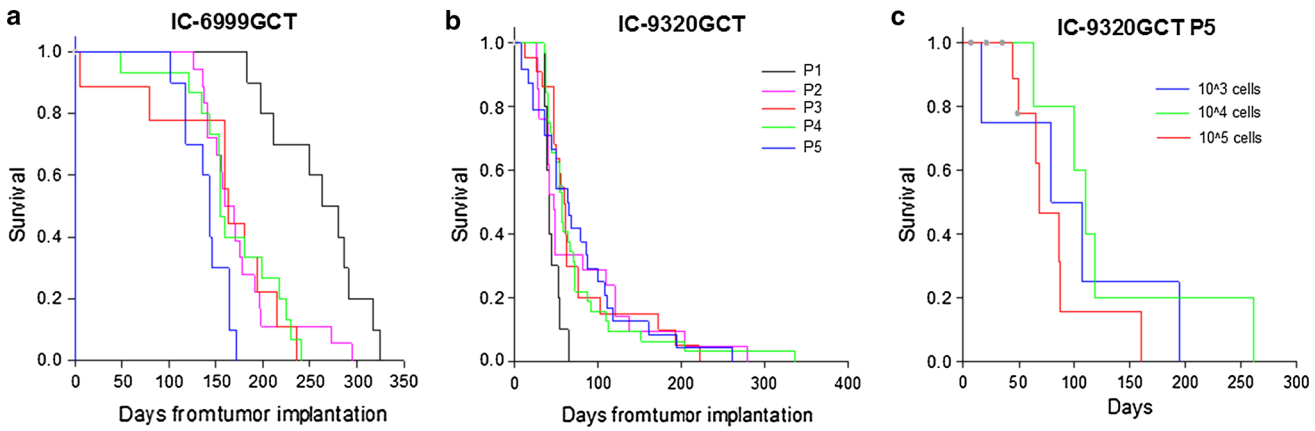

Fig. 1 Germinoma PDOX model survival data. Median survival time of model IC-6999GCT passage 1 (263 days) was significantly different ($p < 0.05$) than passages 2–5 (155 days) (**a**). Median survival time of model IC-9320GCT passages 1 through 5 (53 days) was not significantly different ($p = 0.097$) (**b**). Median survival time of IC-9320GCT passage 5 (86 days) was not significant different with changes in implanted cell number ($p = 0.357$) (**c**)

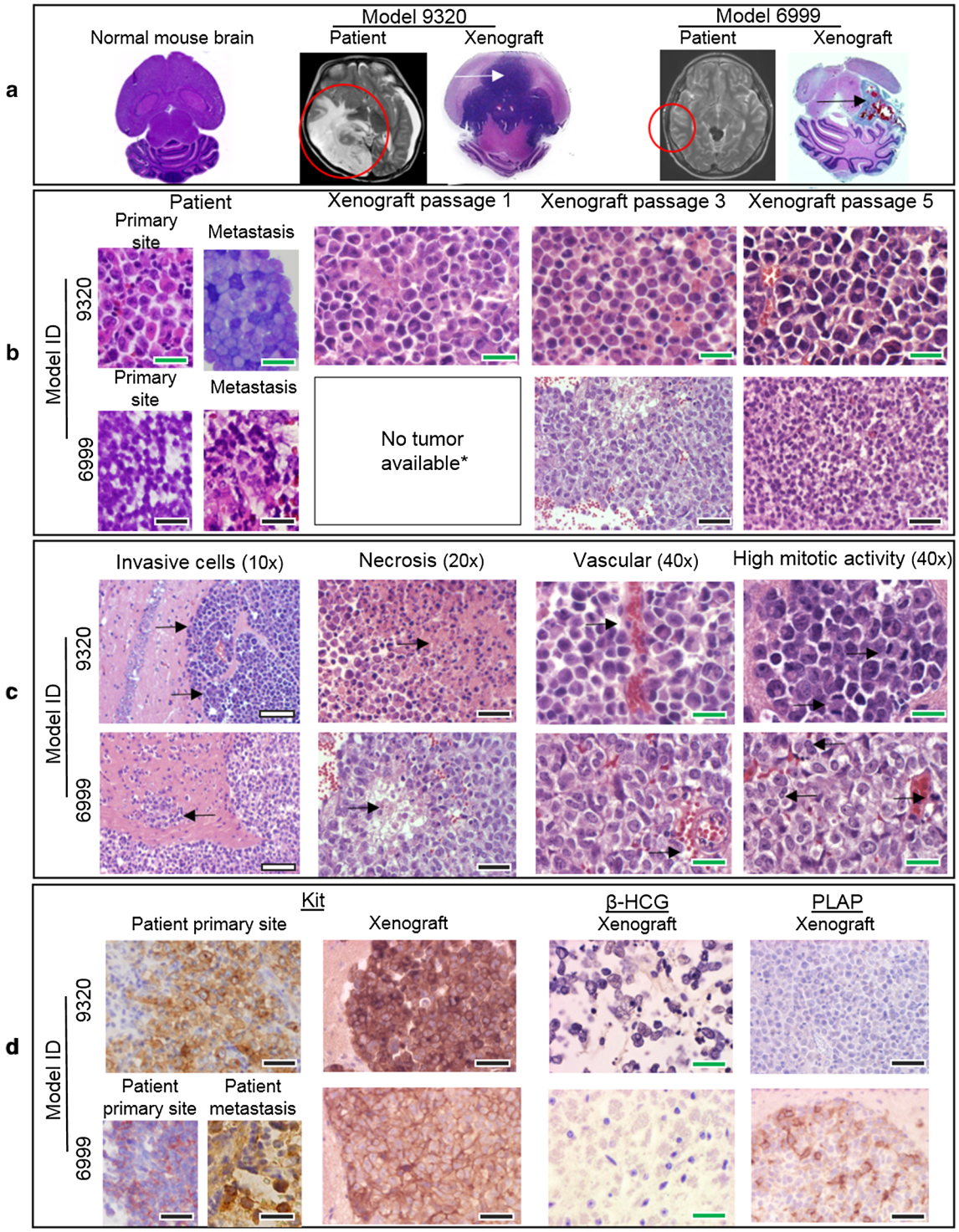

Fig. 2 PDOX model histopathology. H&E whole brain imaging of normal mouse and xenograft models 9320 and 6999 (*arrows* show tumor) with corresponding patient MRI imaging (*circles* show tumor) (**a**). H&E imaging of patient and xenograft tumors from both PDOX models showing tumor cell microscopic similarities (**b**) and malignant features (**c**). IHC imaging of patient and xenograft tumors showing strong (+++) expression of KIT, no expression (−) of β-HCG, and faint expression (+) of PLAP as expected for pure germinoma (**d**). *Scale bars* white = 200 μm, black = 100 μm, green = 50 μm

IC-9320GCT tumors produced an average of 3.4×10^7 live cells per tumor, consistent with the larger size of these tumors compared to those of model IC-6999GCT (Fig. 2a). Live cells from each passage were both sub-transplanted as well as cryopreserved in liquid nitrogen for future use.

As few as 1000 PDOX tumor cells was sufficient to repopulate new xenografts

In order to determine the impact of implanted tumor cell number on xenograft survival times, xenografts of IC-9320GCT passage 5 were injected with the standard 1×10^5 tumor cells as well as both 1×10^3 and 1×10^4 cells. Animal survival times were relatively unchanged (median 86 days) despite the differences in implanted tumor cell number ($p = 0.357$) (Fig. 1c). This suggests that by passage 5, the xenograft model had become well established, with tumor formation occurring even after implantation of only 1×10^3 cells. The results also demonstrate that animal survival times are not solely dictated by implanted tumor cell number but by the tumor's biological characteristics and intrinsic tumorigenicity.

The PDOX tumors replicated the histopathologic and immunohistochemical characteristics of the original patient tumors

Histopathologic and immunohistochemical examination of paraffin-embedded xenograft brains from both tumor models at various passages was performed by our institutional pediatric neuropathologist (A.A.) and confirmed that the xenograft tumors replicated the pathologic phenotypes of the original patient tumors even after 5 in vivo sub-transplantations (Fig. 2). IC-9320GCT tumors were grossly much larger than IC-6999GCT tumors (Fig. 2a). Key histopathologic malignant features including tumor cell invasion, necrosis, and intra-tumoral vascularity were noted in both models and correlated well with findings in the patient tumors (Fig. 2b, c). IHC staining of patient tumors and germinoma models revealed a profile classic for pure germinoma, including strong (+++) expression of KIT, faint expression (+) of PLAP, and no expression (−) of β-HCG (Fig. 2d).

KIT mutation and KIT over-expression were well maintained in the PDOX models

As we recently described, whole-exome sequencing of primary tumor from patient 9320 detected a D816H mutation in *KIT*, with a mutant allele frequency of 14 % [3]. We then performed *KIT* pyrosequencing on the metastatic tumor sample, which detected a mutant allele frequency of 39 % (Fig. 3). To determine the persistence of this mutation throughout serial in vivo sub-transplantations, pyrosequencing was performed on IC-9320GCT xenografts at passages 1–5. Compared to the patient tumor sample, the *KIT* mutation allele frequency was enriched in all xenograft passages (59–70 %) and maintained at a stable fraction over all five sub-transplantations. In contrast, as previously described, primary site tumor from patient 6999 was negative for *KIT* mutation as assessed using targeted deep sequencing with a custom-designed AmpliSeq array [3]. We completed pyrosequencing on the metastatic patient tumor sample, which also did not detect a codon 816 *KIT* mutation; in addition, no mutation was detected in any of the five xenograft passages of model IC-6999GCT (Fig. 3). However, patient and xenograft tumor cells from both models did have overexpression of KIT on IHC staining (Fig. 2d). Since *KIT* is the most frequently mutated gene in CNS germinoma, these models—with and without *KIT* D816H mutation—provide a novel resource for pre-clinical drug testing of targeted therapeutics.

Putative cancer stem cell markers were detected in the PDOX tumors

Xenograft cells from both models at passages 1, 3 and 5 were stained with a panel of established cancer stem cell markers, including CD133, CD15, CD24, CD44 and CD49f, to identify candidate GCT stem cell marker(s) for future functional validation (Fig. 4) [12, 14–24]. Double staining of putative brain tumor stem cell markers CD133 and CD15 detected CD15 mono-positive (CD133−/CD15+) cells both models, ranging from 2 to 4 % in IC-9320GCT and 1–8 % in IC-6999GCT; CD133 mono-positive (CD133+/CD15−) cells, however, were only detected in model IC-6999GCT and with high variability, ranging from 1 % at passage 3–15 % in passage 5 (Fig. 4a). There were no CD133/CD15 double positive cells.

Similarly, CD24 and CD44, markers of breast, colon, and prostate cancer stem cells and found in medulloblastoma and glioma, were analyzed through double staining [14–17, 20]. Although high level (21 %) CD44 mono-positive (CD24−/CD44+) cells were detected in IC-9320GCT at passage 1, these cells decreased to 5 % in passage 3 and 0.5 % in passage 5 (Fig. 4b). Xenograft cells expressing CD24 mono-positive (CD24+/CD44−) or dual positive (CD24+/CD44+) were scarce (<1 % except at passage 3 in IC-9320GCT).

For CD49f, a marker of prostate and breast cancer stem cells[23,24], positive cells were detected in both xenograft models at all analyzed passages (Fig. 4c). There was a steady increase of CD49f+ cells in IC-9320GCT (from 0.4 % in passage 1–4 % in passage 3 and further to 9 % in passage 5) and in IC-6999GCT (from 7 % in passage 1–22 % in passage 5), indicating an active enrichment of CD49f+ cells during serial in vivo passages in mouse brains.

Taken together, this initial screening of putative cancer stem cell markers demonstrated that CD15, CD133, and

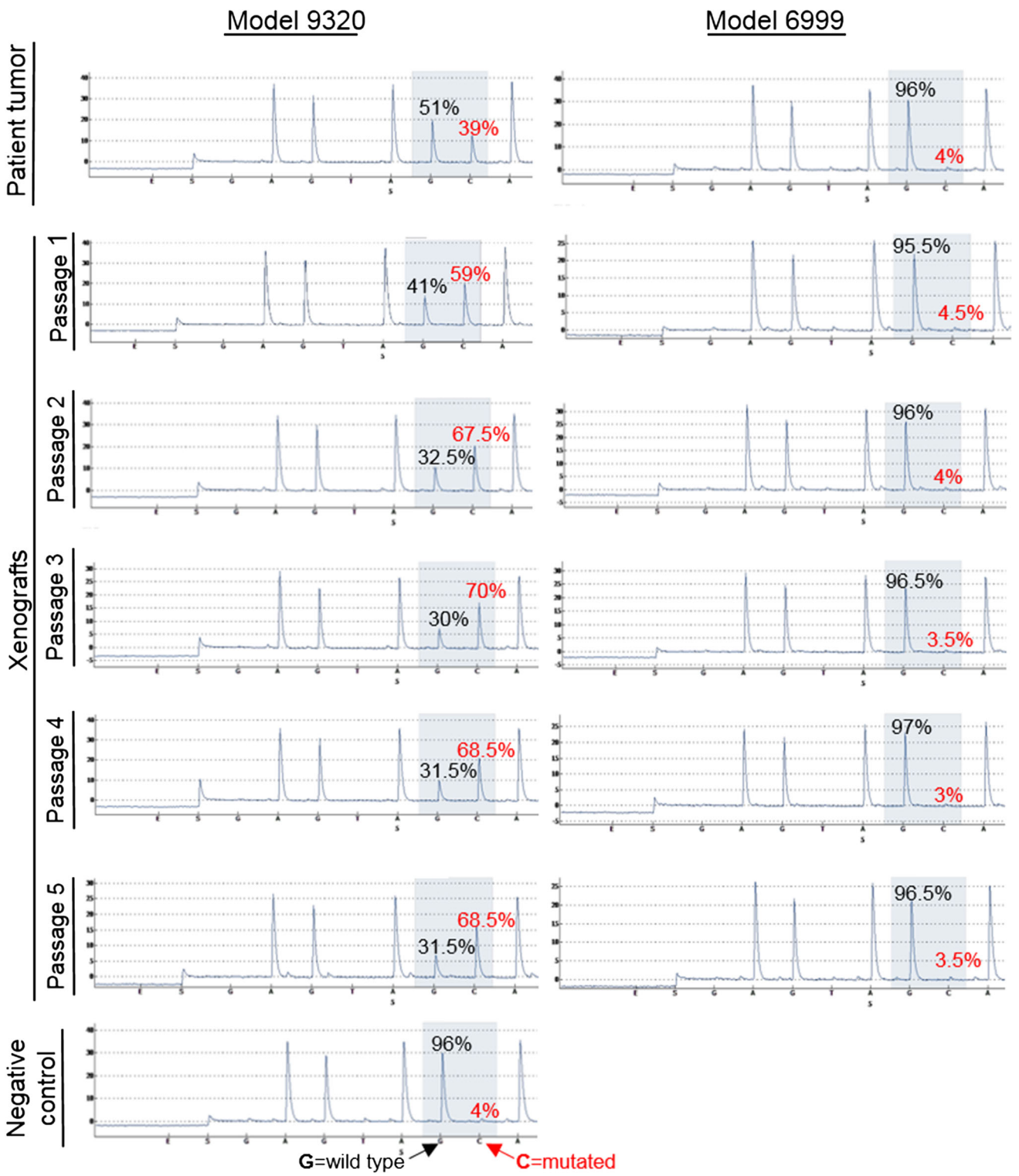

Fig. 3 *KIT* pyrosequencing data. Allele frequency of wild type (*black*) and mutant (*red*) *KIT* in patient and xenograft tumors from both PDOX models

CD49f were expressed in a small population of GCT xenograft tumor cells. As they were detected in both models, CD15+ and CD49f+ GCT cells should be prioritized for future functional analysis of their self-renewal and multi-lineage differentiation capacities to determine if they are truly GCT stem cells.

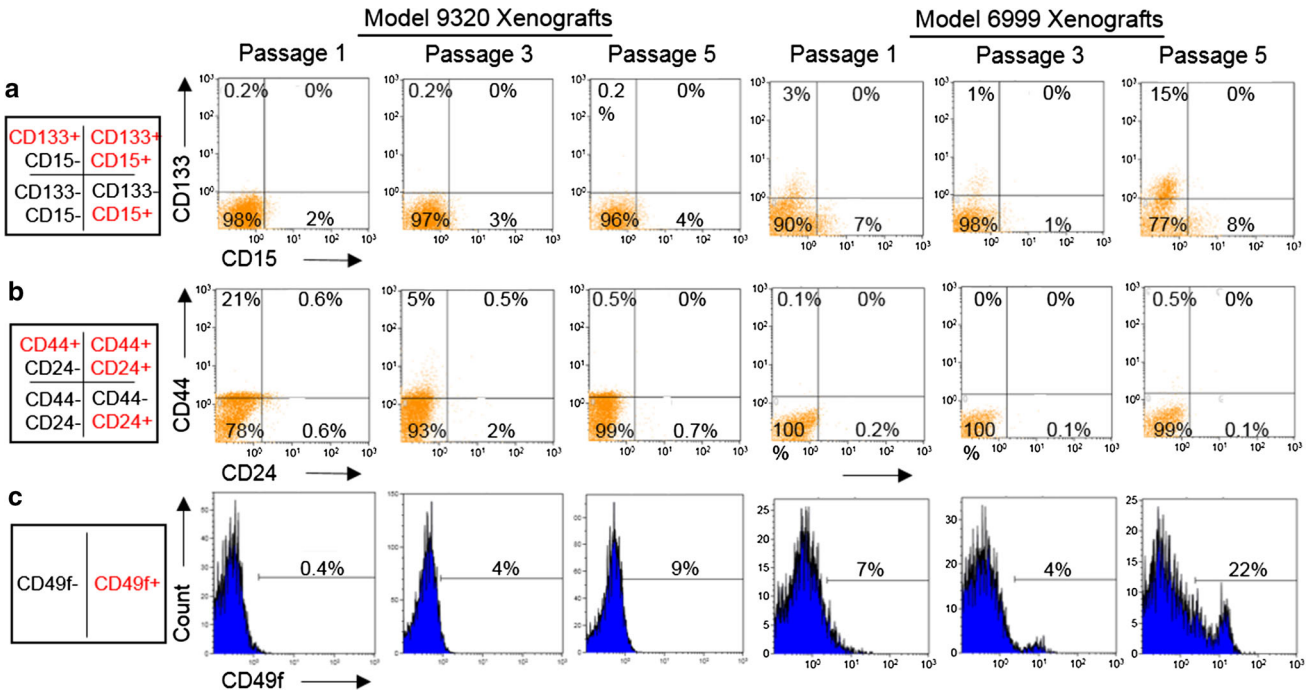

Fig. 4 FACS analysis of candidate germinoma stem cell markers. Xenograft cells of both models at various passages had low but consistent staining for CD15 but not CD133 (other than model 6999 passage 5) across various in vivo passages (**a**). Neither model had significant staining for CD24 or CD44 (other than model 9320 passage 1) (**b**). Both models had low but consistent staining for CD49f (**c**)

Discussion

This study described the establishment of the first two known PDOX models of pediatric intracranial germinoma. These unique germinoma animal models, established from metastatic tumor tissue, replicated the key histopathologic and clinical features of the original patients. We confirmed that KIT over-expression does not require the presence of a mutation (i.e. IC-6999GCT); however, when the mutation is present (i.e. IC-9320GCT), it is not only maintained over serial xenograft passages, but the allele frequency is in fact enriched when compared to the patient tumor.

Surgical resection of intracranial germinoma is rare, with diagnosis typically occurring from tumor biopsy or assessment of tumor markers. Consequently, it is difficult to gain a clear overall pathologic picture of the invasive patterns of this tumor type from patient samples alone. Histopathologic analysis of our xenograft tumors allows a more complete understanding of germinoma invasiveness, vascularity, and mitotic rates throughout various anatomical regions of the tumor.

Furthermore, our data demonstrated that metastatic germinoma cells can form xenograft tumors from the intracranial implantation of as few as 1000 cells. In addition, tumor-induced animal death occurs in the same time frame for mice injected with 1×10^3, 1×10^4, and 1×10^5 germinoma cells. These foreboding findings underscore the fact that the goal of anti-neoplastic therapy must be to kill all malignant cells, not simply the majority, in order to eliminate the tumor and provide meaningful extension of patient survival. In addition, we showed that KIT overexpression can occur independently of *KIT* D816H mutation (i.e. IC-6999GCT). As *KIT* is the most commonly mutated gene in intracranial germinoma and KIT over-expression a pathologic characteristic of these tumors, our PDOX models—one with *KIT* mutation and both with KIT over-expression—are excellent representations of the genomic and pathologic spectrum of CNS germinomas.

These models represent both untreated (IC-9320GCT) and previously-treated (IC-6999GCT) tumors. This novel pair of GCT PDOX models thus provides an opportunity to evaluate the role of new therapeutics both in untreated and pre-treated/relapsed GCT.

Our data identified CD15 and CD49f as candidate cell surface markers of intracranial germinoma stem cells given their presence at low but consistent levels in both PDOX models. Although only two patient tumors were analyzed, the stability of CD49f and CD15 expression throughout serial in vivo tumor sub-transplantations supports our conclusion that these cell surface molecules should be highly ranked as candidate CNS germinoma stem cell markers for future functional validation studies.

Our PDOX models do have limitations. As the tumors are implanted into SCID mice, the models do not allow assessments of tumor immunology or investigations of immuno-therapies. In addition, we implanted germinoma tumor cells in the mouse cerebra due to the significant technical difficulty of implantation into the midbrain, the most common site of these tumors. Finally, our PDOX models have lengthy survival times and that there is a significant difference in average survival time between the two models. However, we feel that this in fact accurately reflects the widely variable clinical phenotype of germinomas.

Overall, these newly established orthotopic xenograft models of metastatic pediatric intracranial germinoma meet the critical research and clinical need for well characterized in vivo systems in which to pre-clinically test new therapeutic agents.

References

1. Osorio DS, Finlay JL, Dhall G, Goldman S, Eisenstat D, Brown RJ (2013) Feasibility of dasatinib in children and adolescents with new or recurrent central nervous system germinoma. Pediatr Blood Cancer 60:E100–E102. doi:10.1002/pbc.24567
2. Murray MJ, Horan G, Lowis S, Nicholson JC (2013) Highlights from the Third International Central Nervous System Germ Cell Tumour symposium: laying the foundations for future consensus. Ecancermedicalscience 7:333. doi:10.3332/ecancer.2013.333
3. Wang L, Yamaguchi S, Burstein MD, Terashima K, Chang K, Ng HK, Nakamura H, He Z, Doddapaneni H, Lewis L, Wang M, Suzuki T, Nishikawa R, Natsume A, Terasaka S, Dauser R, Whitehead W, Adekunle A, Sun J, Qiao Y, Marth G, Muzny DM, Gibbs RA, Leal SM, Wheeler DA, Lau CC (2014) Novel somatic and germline mutations in intracranial germ cell tumours. Nature 511:241–245. doi:10.1038/nature13296
4. Echevarria ME, Fangusaro J, Goldman S (2008) Pediatric central nervous system germ cell tumors: a review. Oncologist 13:690–699. doi:10.1634/theoncologist.2008-0037
5. Jackson C, Jallo G, Lim M (2011) Clinical outcomes after treatment of germ cell tumors. Neurosurg Clin North Am 22(3):385–394. doi:10.1016/j.nec.2011.04.002
6. Sakuma Y, Sakurai S, Oguni S, Satoh M, Hironaka M, Saito K (2004) c-kit gene mutations in intracranial germinomas. Cancer Sci 95:716–720
7. Kamakura Y, Hasegawa M, Minamoto T, Yamashita J, Fujisawa H (2006) C-kit gene mutation: common and widely distributed in intracranial germinomas. J Neurosurg 104:173–180. doi:10.3171/ped.2006.104.3.173
8. Fukushima S, Otsuka A, Suzuki T, Yanagisawa T, Mishima K, Mukasa A, Saito N, Kumabe T, Kanamori M, Tominaga T, Narita Y, Shibui S, Kato M, Shibata T, Matsutani M, Nishikawa R, Ichimura K, On behalf of the Intracranial Germ Cell Tumor Genome Analysis C (2014) Mutually exclusive mutations of KIT and RAS are associated with KIT mRNA expression and chromosomal instability in primary intracranial pure germinomas. Acta Neuropathol. doi:10.1007/s00401-014-1247-5
9. Demetri GD, von Mehren M, Blanke CD, Van den Abbeele AD, Eisenberg B, Roberts PJ, Heinrich MC, Tuveson DA, Singer S, Janicek M, Fletcher JA, Silverman SG, Silberman SL, Capdeville R, Kiese B, Peng B, Dimitrijevic S, Druker BJ, Corless C, Fletcher CD, Joensuu H (2002) Efficacy and safety of imatinib mesylate in advanced gastrointestinal stromal tumors. New Engl J Med 347:472–480. doi:10.1056/NEJMoa020461
10. Chen H, Isozaki K, Kinoshita K, Ohashi A, Shinomura Y, Matsuzawa Y, Kitamura Y, Hirota S (2003) Imatinib inhibits various types of activating mutant kit found in gastrointestinal stromal tumors. Int J Cancer J Int Du Cancer 105:130–135. doi:10.1002/ijc.11025
11. Yu L, Baxter PA, Voicu H, Gurusiddappa S, Zhao Y, Adesina A, Man TK, Shu Q, Zhang YJ, Zhao XM, Su JM, Perlaky L, Dauser R, Chintagumpala M, Lau CC, Blaney SM, Rao PH, Leung HC, Li XN (2010) A clinically relevant orthotopic xenograft model of ependymoma that maintains the genomic signature of the primary tumor and preserves cancer stem cells in vivo. Neuro-Oncology 12:580–594. doi:10.1093/neuonc/nop056
12. Shu Q, Wong KK, Su JM, Adesina AM, Yu LT, Tsang YT, Antalffy BC, Baxter P, Perlaky L, Yang J, Dauser RC, Chintagumpala M, Blaney SM, Lau CC, Li XN (2008) Direct orthotopic transplantation of fresh surgical specimen preserves CD133+ tumor cells in clinically relevant mouse models of medulloblastoma and glioma. Stem Cells 26:1414–1424. doi:10.1634/stemcells.2007-1009
13. Gao Y, Jiang J, Liu Q (2014) Clinicopathological and immunohistochemical features of primary central nervous system germ cell tumors: a 24-years experience. Int J Clin Exp Pathol 7:6965–6972
14. Liu Z, Zhao X, Wang Y, Mao H, Huang Y, Kogiso M, Qi L, Baxter PA, Man TK, Adesina A, Su JM, Picard D, Ching Ho K, Huang A, Perlaky L, Lau CC, Chintagumpala M, Li XN (2014) A patient tumor-derived orthotopic xenograft mouse model replicating the group 3 supratentorial primitive neuroectodermal tumor in children. Neuro-Oncology 16:787–799. doi:10.1093/neuonc/not244
15. Anido J, Saez-Borderias A, Gonzalez-Junca A, Rodon L, Folch G, Carmona MA, Prieto-Sanchez RM, Barba I, Martinez-Saez E, Prudkin L, Cuartas I, Raventos C, Martinez-Ricarte F, Poca MA, Garcia-Dorado D, Lahn MM, Yingling JM, Rodon J, Sahuquillo J, Baselga J, Seoane J (2010) TGF-beta receptor inhibitors target the CD44(high)/Id1(high) glioma-initiating cell population in human glioblastoma. Cancer Cell 18:655–668. doi:10.1016/j.ccr.2010.10.023
16. Visvader JE, Lindeman GJ (2008) Cancer stem cells in solid tumours: accumulating evidence and unresolved questions. Nat Rev Cancer 8:755–768. doi:10.1038/nrc2499
17. Fillmore C, Kuperwasser C (2007) Human breast cancer stem cell markers CD44 and CD24: enriching for cells with functional properties in mice or in man? Breast Cancer Res: BCR 9:303. doi:10.1186/bcr1673
18. Cheng JX, Liu BL, Zhang X (2009) How powerful is CD133 as a cancer stem cell marker in brain tumors? Cancer Treat Rev 35:403–408. doi:10.1016/j.ctrv.2009.03.002
19. Singh SK, Clarke ID, Terasaki M, Bonn VE, Hawkins C, Squire J, Dirks PB (2003) Identification of a cancer stem cell in human brain tumors. Cancer Res 63:5821–5828
20. Sanden E, Dyberg C, Krona C, Visse E, Caren H, Northcott PA, Kool M, Stahl N, Persson A, Englund E, Johnsen JI, Siesjo P, Darabi A (2015) Aberrant immunostaining pattern of the CD24 glycoprotein in clinical samples and experimental models of pediatric medulloblastomas. J Neurooncol 123:1–13. doi:10.1007/s11060-015-1758-5
21. Read TA, Fogarty MP, Markant SL, McLendon RE, Wei Z, Ellison DW, Febbo PG, Wechsler-Reya RJ (2009) Identification of CD15 as a marker for tumor-propagating cells in a mouse model of medulloblastoma. Cancer Cell 15:135–147. doi:10.1016/j.ccr.2008.12.016

22. Mao XG, Zhang X, Xue XY, Guo G, Wang P, Zhang W, Fei Z, Zhen HN, You SW, Yang H (2009) Brain tumor stem-like cells identified by neural stem cell marker CD15. Transl Oncol 2:247–257
23. Yamamoto H, Masters JR, Dasgupta P, Chandra A, Popert R, Freeman A, Ahmed A (2012) CD49f is an efficient marker of monolayer- and spheroid colony-forming cells of the benign and malignant human prostate. PLoS One 7:e46979. doi:10.1371/journal.pone.0046979
24. Atkinson RL, Yang WT, Rosen DG, Landis MD, Wong H, Lewis MT, Creighton CJ, Sexton KR, Hilsenbeck SG, Sahin AA, Brewster AM, Woodward WA, Chang JC (2013) Cancer stem cell markers are enriched in normal tissue adjacent to triple negative breast cancer and inversely correlated with DNA repair deficiency. Breast Cancer Res: BCR 15:R77. doi:10.1186/bcr3471